 doi: 10.18287/JBPE21.07.020306A

Appendix: Optical Signature Analysis of Liver Ablation Stages Exploiting Spatio-Spectral Imaging

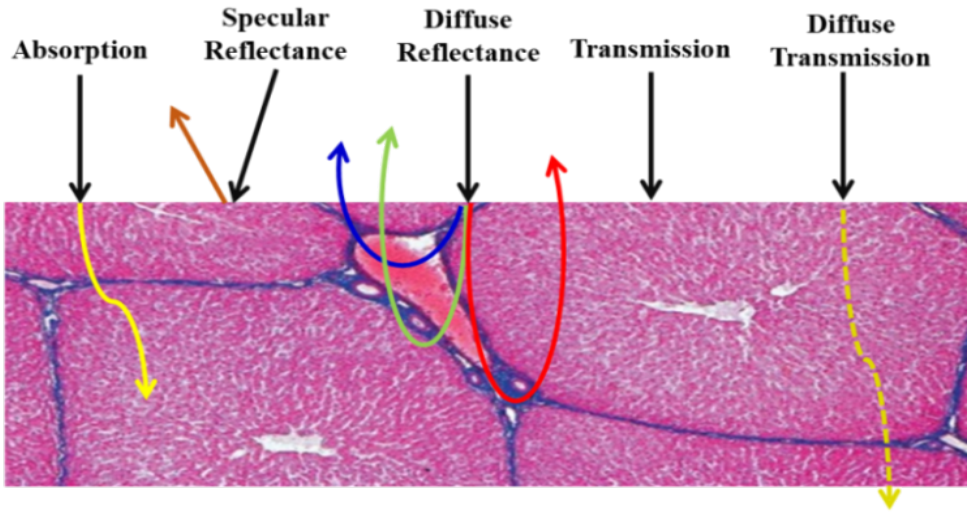

Fig. A1 Demonstration for the *ex vivo* Liver Tissue from a bovin for the optical properties (transmission, reflection, absorption, and scattering) over the various spectrum ranges.

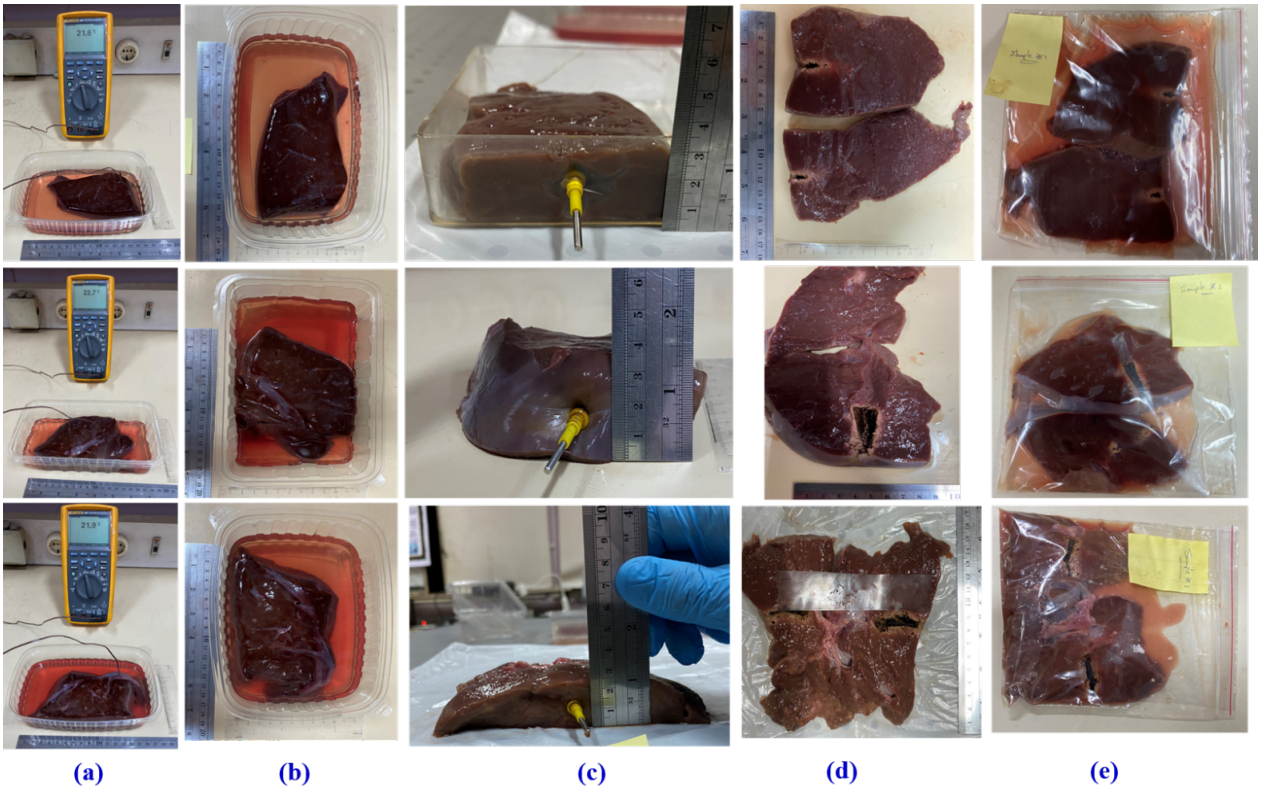

Fig. A2 (From Up to Down) The investigated liver Sample #5, liver Sample #6, and liver Sample #7; (a) the investigated liver sample before ablation inserted in neutral buffered saline and observed with a multimeter (Fluke, 289, USA), (b) the investigated liver sample inserted in the neutral buffered saline for tissue size recording, (c) the investigated liver sample after ablation in the experimental plastic tray with the active RF tip inserted in the sample, (d) the investigated liver sample after ablation and slicing to compare the actual ablated region and recording the size by scientific expert, (e) the sliced liver Sample #2 after ablation and wrapped in the vacuumed bags and tissue storage solution prepared to be sent to the pathological lap.

Table A1 The experimental data of the investigated liver tissue samples with the power protocol and duration for each experiment and the actual measured of the ablation region after sample slicing.

No.	Liver Sample Identification	Sample Size L×W, cm	Tissue Thickness h, cm	Position of RF Tip, cm	RF generator Power, W	Time of Ablation, min	Size of Ablation L×W, cm
1	Sample #1	10.1×9.5	2.8	1.5	35	2.5	1.9×0.7
2	Sample #2	9.1×10.5	2.3	1.5	35	4	2.1×0.8
3	Sample #3	11.1×10.2	2.7	1.5	30	5	3.1×1.3
4	Sample #4	15.1× 9.5	3.1	2	25	2	1.1×0.41
5	Sample #5	16×10.6	3.6	1.5	40	2.3	4×1.2
6	Sample #6	17×9	2.5	1.5	50	3.5	4.7×1.3
7	Sample #7	9.2×9.5	2.3	1.5	35	2	2.1×0.8

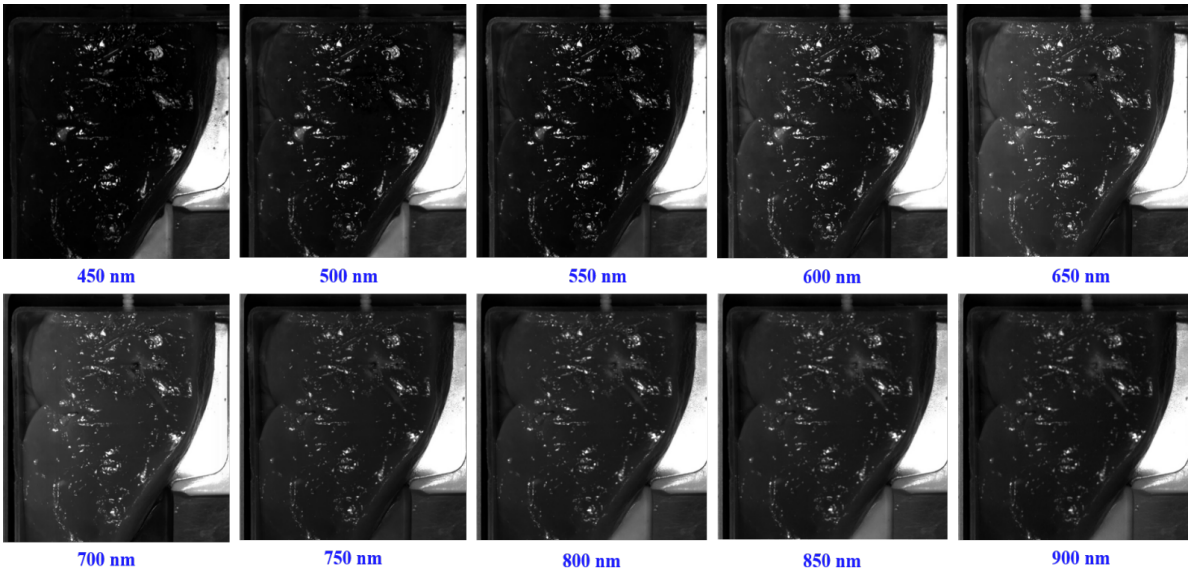

Fig. A3 The scanned HS images of the investigated *ex vivo* liver Sample #4 after ablation from 450 nm till 900 nm with 50 nm resolution, where we could visually see the differentiation of the ablation and thermal effect regions on the various HS images in the spectral range.

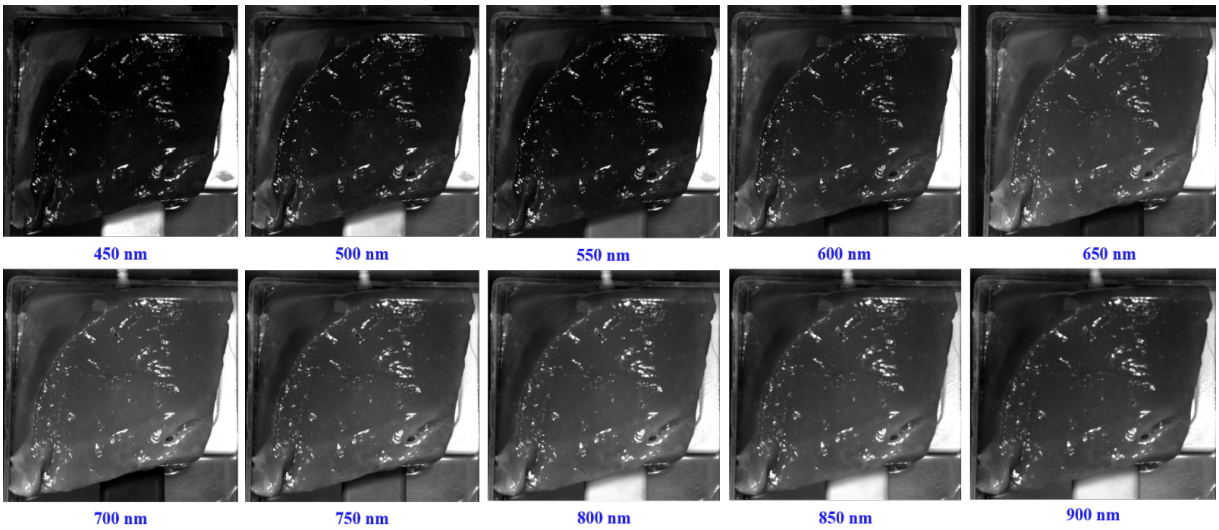

Fig. A4 The scanned HS images of the investigated *ex vivo* liver Sample #5 after ablation from 450 nm till 900 nm with 50 nm resolution, where we could visually see the differentiation of the ablation and thermal effect regions on the various HS images in the spectral range.

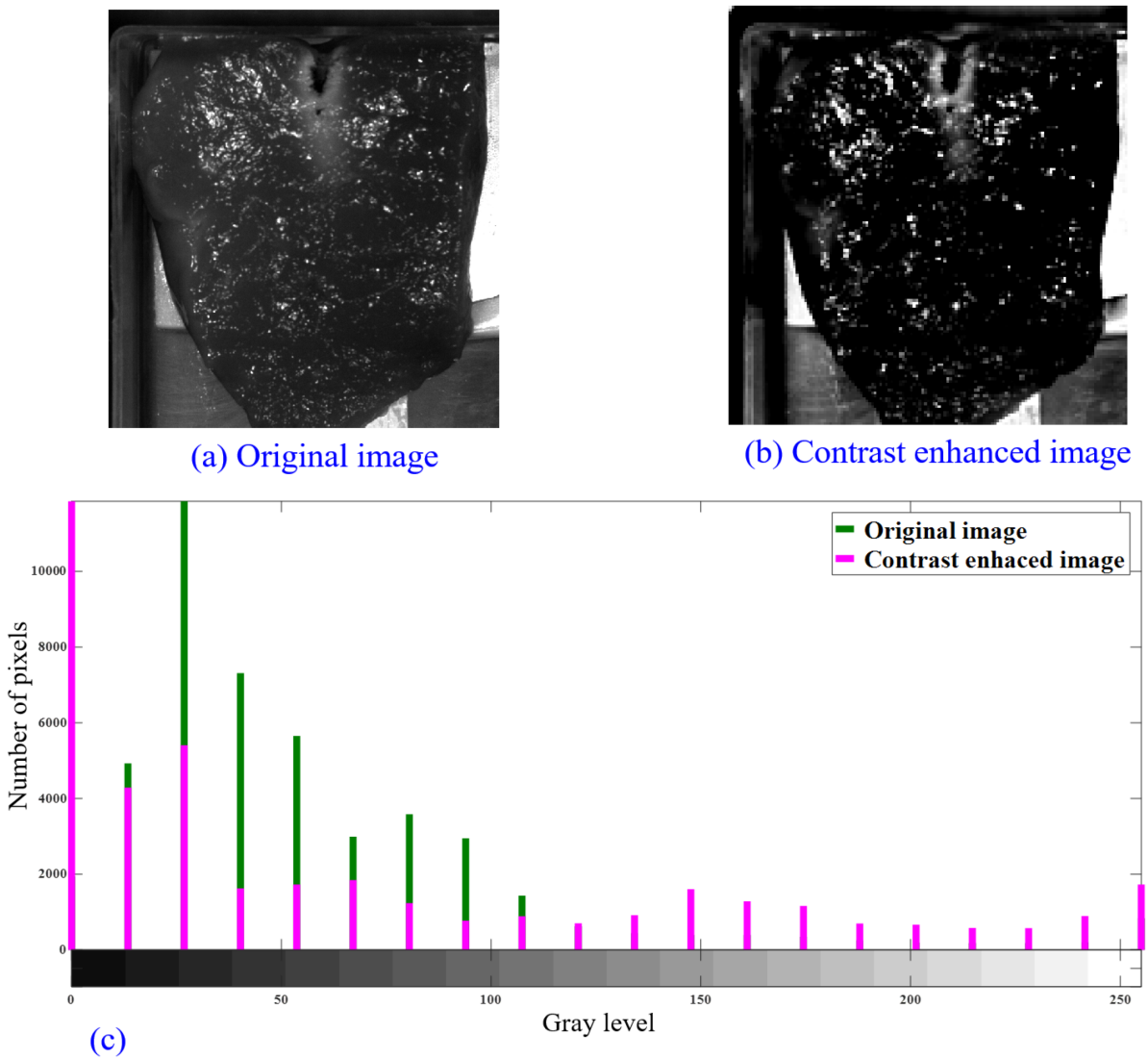

Fig. A5 The original image at wavelength 900 nm of the investigated Liver tissue Sample #4 after ablation and slicing but before image contrast enhancement; (b) the enhanced image contrast utilizing the "Top-hat and Bottom-hat transforms"; (c) the histogram which weveals the contrast of the original image with the green bars and the enhanced image contrast with the purple bars.

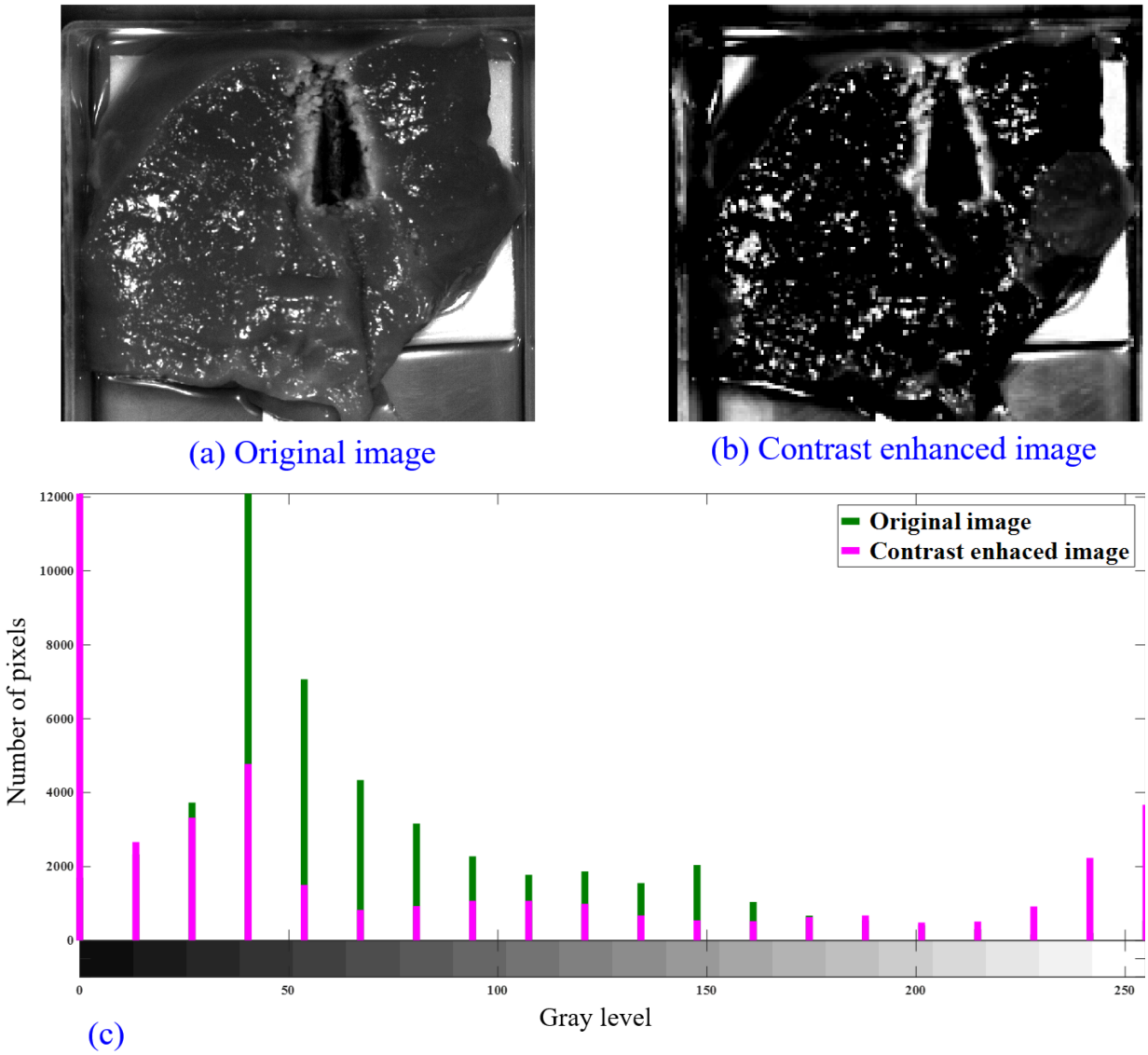

Fig. A6 The original image at wavelength 900 nm of the investigated liver tissue Sample#5 after ablation and slicing but before image contrast enhancement; (b) the enhanced image contrast utilizing the "Top-hat and Bottom-hat transforms"; (c) the histogram which reveals the contrast of the original image with the green bars and the enhanced image contrast with the purple bars.

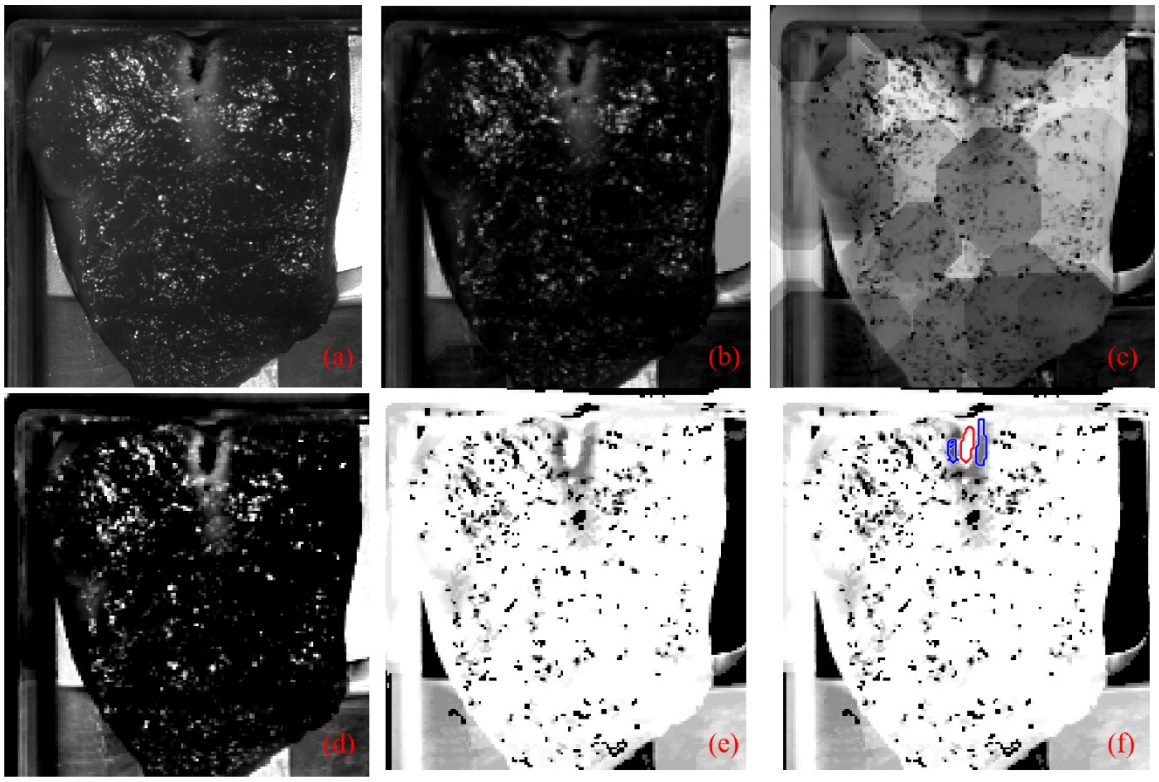

Fig. A7 The investigated liver tissue Sample #4 after thermal ablation and slicing; (a) the acquired hyperspectral image at 900 nm; (b) the image contrast enhancement after top-hat transforms; (c) the image contrast enhancement after bottom-hat transforms; (d) the enhanced contrast image; (e) the final complement enhancement image; (f) the delineation contour for the ablation and thermally affected region in red and blue, respectively.

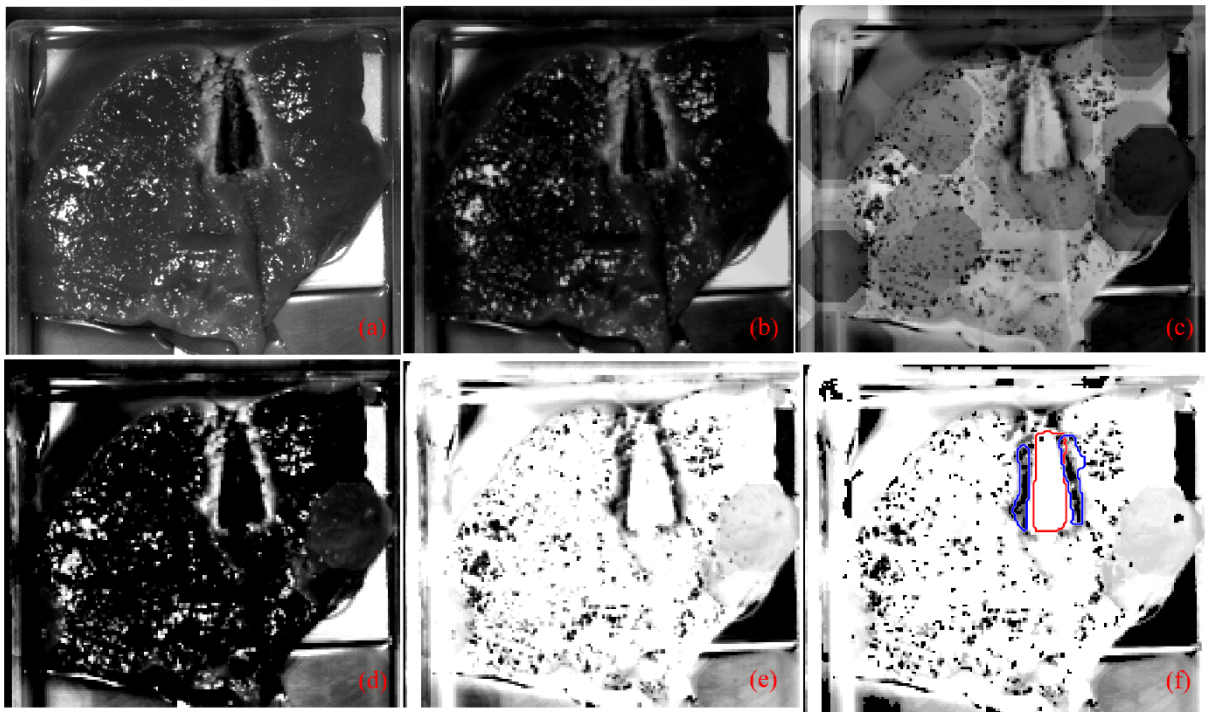

Fig. A8 The investigated liver tissue Sample#5 after thermal ablation and slicing; (a) the acquired hyperspectral image at 900 nm; (b) the image contrast enhancement after top-hat transforms; (c) the image contrast enhancement after bottom-hat transforms; (d) the enhanced contrast image; (e) the final complement enhancement image; (f) the delineation contour for the ablation and thermally affected region in red and blue, respectively.

A stable light source is very important to achieve usable measurement information, also to ensure measurement repeatability, and affecting the accuracy of the HS camera. We aimed to measure the light diffuse reflectance (R_d) for an *ex-vivo* liver tissue samples, by exploring the optical properties spectroscopy in the near-infrared and visible (NIR-VIS) spectrum. Where, the utilized light assembly for our hyperspectral imaging (HSI) system, a power supply controller for the source light (Mean Well, ENP360-12, Taiwan) with a polychromatic light source (4 × 35 W tungsten halogen lamps) at wavelength range (380~1050 nm), as shown in Figure A9.

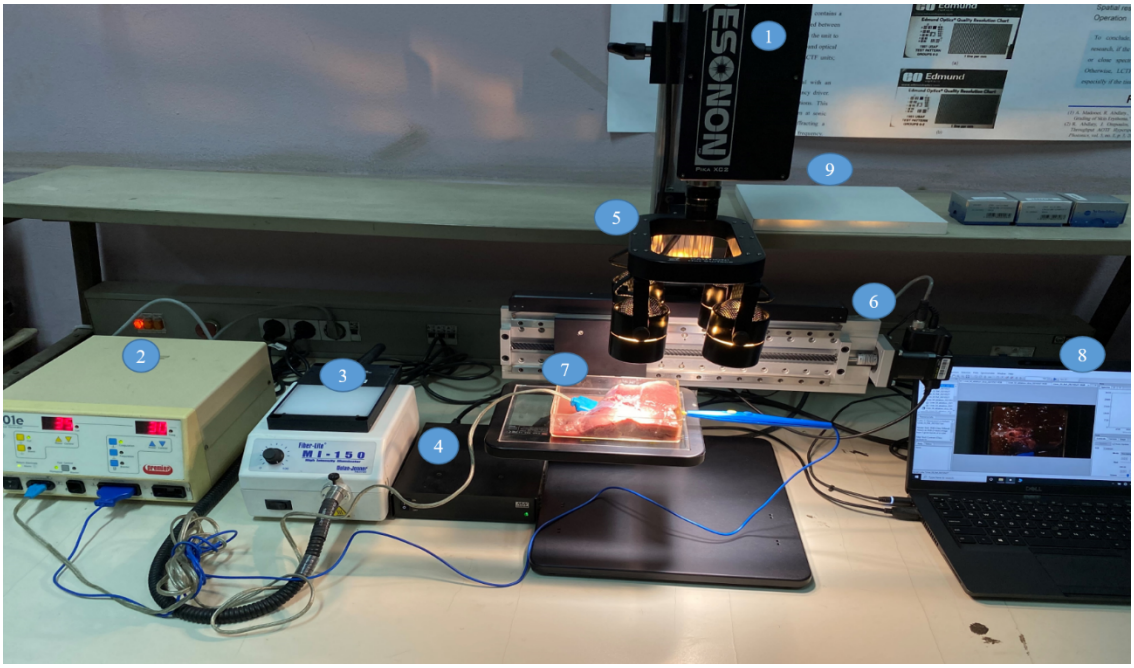

Fig. A9 Hyperspectral Optical Imaging system for measuring the light diffuse reflectance (R_d) of the investigated *ex-vivo* tissue samples; (1) Hyperspectral camera (Resonon, Pika XC2, USA); (2) Electrosurgical Generator (Premier; 2001e, France); (3) The Source light for the transmission measurement trials (Fiber-lite, MI-150, USA); (4) The power supply controller for the light source (Mean Well, ENP360-12, Taiwan) of diffuse reflection (R_d) measurement trails; (5) The 4-Halogen lamps (4 × 35 W halogen lamps) at wavelength range (380~1050 nm); (6) the linear translation stage; (7) The investigated *ex-vivo* liver sample; (8) The computer and Image Software Processing and Analysis, (9) white tile with high reflectance (Avian Technologies, FWT-99-300R058, UK).

The tungsten halogen incandescent lamps are thermal radiators. Where, light is generated by heating a solid body up to a high temperature, as temperature increase leading to more luminous light, and inversely for the wavelength (The melting point of tungsten (3383 °C) does not allow the peak to be shifted into the visible, about 20% of the total radiation is given off as “light”, about 0.3% in the UV region, and the remaining majority as heat) [1].

This type of lamps, generates a continuous distribution of light across the visible spectrum, although most of the energy emitted by these lamps is dissipated as heat in the infrared (IR) wavelengths. Due to their relatively weak emission in the ultraviolet portion of the spectrum, tungsten-halogen lamps are not as useful as arc lamps and lasers for examining specimens that must be illuminated with wavelengths below 400 nm [2], as illustrated in Figure A10.

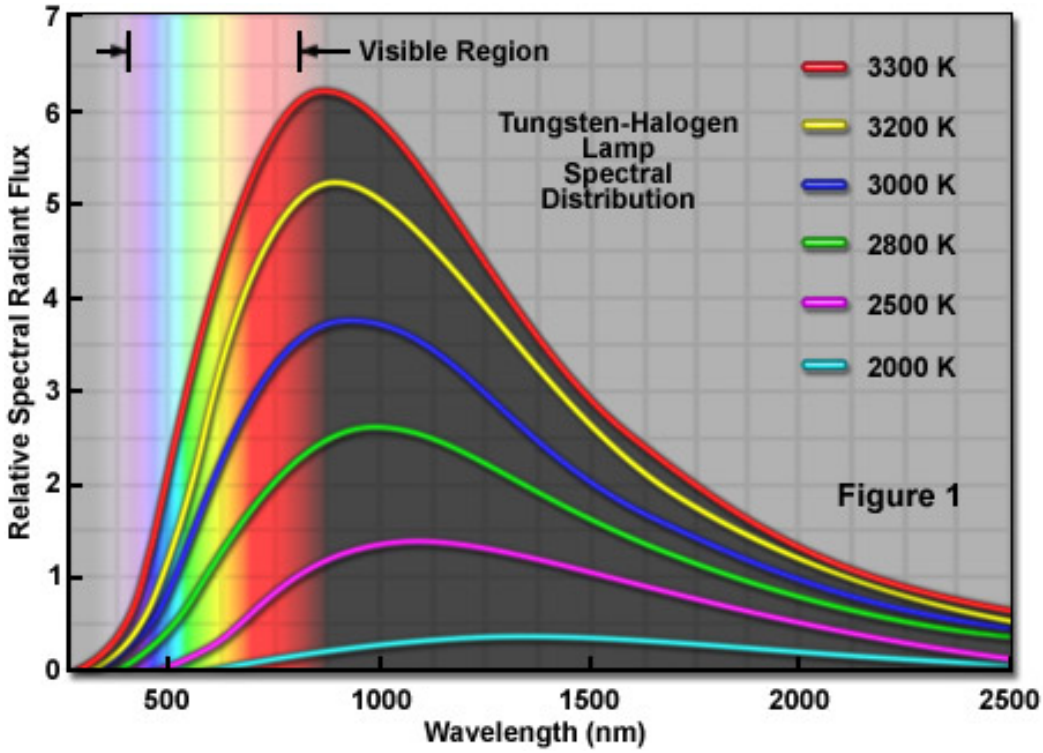

Fig. A10 The spectral distribution of the tungsten halogen incandescent lamps illustrates as temperature increase leading to more luminous light and shorter wavelength and the heat dissipation in the direction of the infrared (IR) wavelengths.

Furthermore, during the warm-up time, tungsten halogen light sources normally alter their spectral power distribution and release considerable amount of energy by way of heat, IR. Throughout this warm-up period, an increasing amount of IR promotes changes in the spectral power distribution and results may differ when measurements are taken during this time. Hence, it is recommended that the light source is allowed to stabilize for about 3-5 minutes [3]. In the presented study we maintain a considerable time about ~3 minutes (warming in advance of the investigation sample capturing), and not to exceed the reasonable warming time to avoid the heat effect on the investigated samples.

Additionally, in the NIR and VIS region, if the wavelength is longer, its signal/noise ratio would be relatively better for measurements. Such types of light sources are ideal for reflective and transmissive measurements in the VIS-NIR's longer wavelengths [2,3]. As in our investigation, we aim to measure the light (R_d), that's why we chose this specifically HS camera model (Resonon, Pika XC2, USA) with spectral range (400-1000 nm), as displayed in Figure A11.

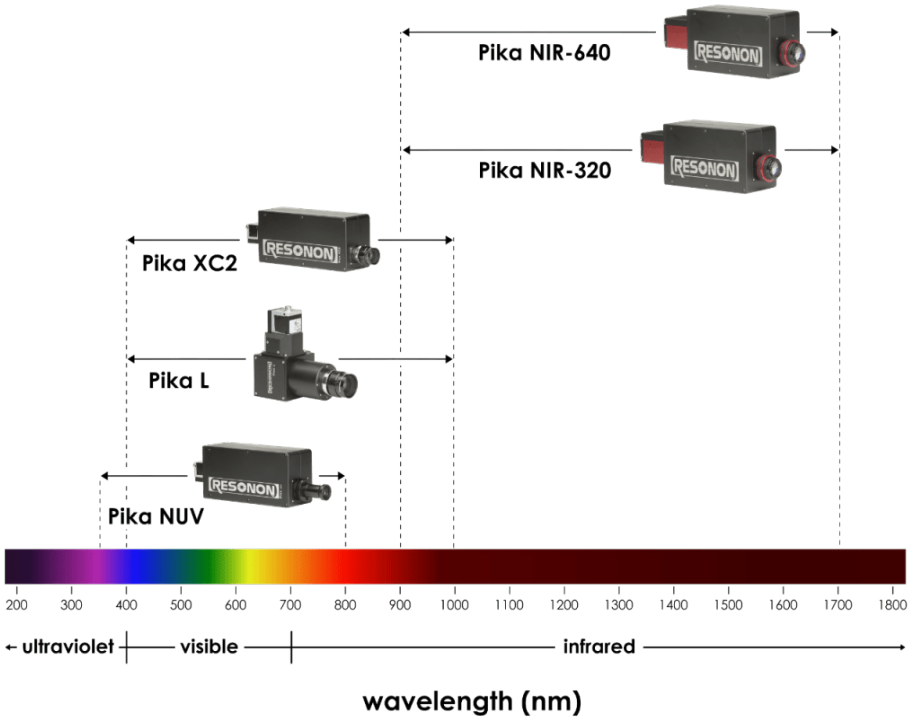

Fig. A11 The different models of the Resonon HS camera identifying the various spectrum wavelength.

Finally, at the startup of each investigation, and before capturing the investigated samples, we measure the light diffuse reflectance (Ṛd) of the highly reflectance white board (Avian Technologies, FWT-99-300R058, UK) to be our reference, as indicated with No# 1 in Figure A9.

References

[1] J.. Coaton, Halogen light sources Operating tungsten halogen lamps Halogen light sources Operating tungsten halogen lamps, 9(1) (1977) 25–30.
[2] A. Ożarowski, National High Magnetic Field Laboratory, Florida State University, 1800 E, Paul Dirac Drive, Tallahassee, Florida. 32310 (n.d.).
[3] A. V Arecchi, R.J. Koshel, T. Messadi, Field guide to illumination, in: SPIE, 2007.